J. Biophoton. **2**, No. 3, 145–156 (2009) / **DOI** 10.1002/jbio.200810040

Journal of BIOPHOTONICS

FULL ARTICLE

Mueller matrix decomposition for polarized light assessment of biological tissues

Nirmalya Ghosh[**,1] *Michael F. G. Wood*[**,1], *Shu-hong Li*[2], *Richard D. Weisel*[2], *Brian C. Wilson*[1], *Ren-Ke Li*[2], *and I. Alex Vitkin*[3,*]

[1] Ontario Cancer Institute, Division of Biophysics and Bioimaging, University Health Network, Toronto, Ontario, Canada; University of Toronto, Department of Medical Biophysics, Toronto, Ontario, Canada.
[2] Toronto General Research Institute, Division of Cardiovascular Surgery, Toronto, Ontario, Canada; Toronto General Hospital, Division of Cardiac Surgery, Toronto, Ontario, Canada; University of Toronto, Toronto, Ontario, Canada.
[3] Ontario Cancer Institute, Division of Biophysics and Bioimaging, University Health Network, Toronto, Ontario, Canada; University of Toronto, Department of Medical Biophysics and Radiation Oncology, Toronto, Ontario, Canada.

Received 8 July 2008, revised 15 August 2008, accepted 7 October 2008
Published online 24 October 2008

Key words: polarimetry, optical activity, birefringence, non-invasive tissue characterization, glucose, regenerative medicine

The Mueller matrix represents the transfer function of an optical system in its interactions with polarized light and its elements relate to specific biologically or clinically relevant properties. However, when many optical polarization effects occur simultaneously, the resulting matrix elements represent several "lumped" effects, thus hindering their unique interpretation. Currently, no methods exist to extract these individual properties in turbid media. Here, we present a novel application of a Mueller matrix decomposition methodology that achieves this objective. The methodology is validated theoretically via a novel polarized-light propagation model, and experimentally in tissue simulating phantoms. The potential of the approach is explored for two specific biomedical applications: monitoring of changes in myocardial tissues following regenerative stem cell therapy, through birefringence-induced retardation of the lights linear and circular polarizations, and non-invasive blood glucose measurements through chirality-induced rotation of the lights linear polarization. Results demonstrate potential for both applications.

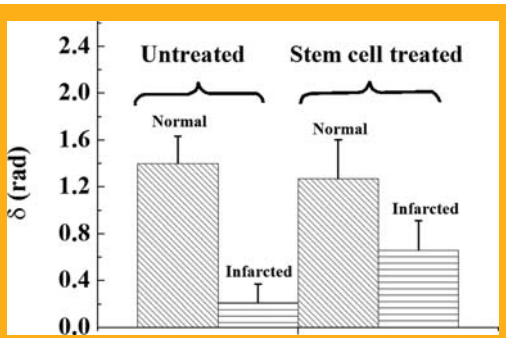

Birefringence measurements in normal and infarcted regions of ex vivo untreated and stem cell treated rat myocardium. Note the higher birefringence values in the infarcted region with treatment

1. Introduction

Polarimetry has played important roles in understanding the nature of electromagnetic waves [1], elucidating the three dimensional characteristics of chemical bonds [2], uncovering the asymmetric (chiral) nature of biological molecules [3], determining sugar concentrations in industrial processes [4], quantifying

* Corresponding author: e-mail: vitkin@uhnres.utoronto.ca
** Nirmalya Ghosh and Michael F. G. Wood contributed equally to this work.

protein properties in solutions [5], supplying a variety of nondestructive evaluation methods [6], developing advanced concepts such as polarization entropy [7], contributing to remote sensing in meteorology and astronomy [8, 9], differentiating between normal and pre-cancerous cells [10], as well as other biomedical applications [11, 12]. Traditional polarimetry is well suited for applications in optically clear media and for studies of surfaces; however, multiple scattering in optically thick turbid media such as most biological tissues causes extensive depolarization that confounds the established techniques. Further, even if some residual polarization signal can be measured [13], multiple scattering also alters the polarization state, for example by scattering-induced diattenuation [14] and by scattering-induced changes in the orientation of the linear polarization vector which appears as optical rotation [15]. Other simultaneously occurring polarization effects further confound quantitative polarimetry in complex materials; in tissues, these include linear birefringence due to anisotropic muscle fibers and structural proteins, and optical rotation due to optically active (chiral) molecules and structures. Thus, although a wealth of interesting tissue properties can potentially be probed with polarized light, accurate measurements and data analyses leading to unique interpretation of the polarization parameters are difficult. Hence, a method to account for the effects of multiple scattering, and to decouple the individual contributions of several effects occurring simultaneously is needed. Although recent work has shown promise for empirically extracting semi-quantitative information and relative changes from thick random media under controlled conditions [16–29], a more quantifiable and generally applicable technique is required. Here, we describe such a generalized method for polarimetry analysis in turbid media based on polar Mueller matrix decomposition. In addition, we present preliminary results for the use of this methodology for non-invasive tissue glucose measurements and monitoring regenerative treatments of myocardial infarction.

2. Methods and materials

2.1. Mueller algebra

The polarization of light is well described either via Jones or Mueller matrix algebra [30], although the latter is preferred when dealing with depolarizing interactions as engendered by multiply scattering media. Using the Mueller matrix approach, the intensity and polarization of a light beam are represented by a 4-element Stokes vector, **S**. The first element I represents the intensity of the light beam, the second element Q represents the linear polarization at 0° and 90°, the third element U represents the linear polarization at 45° and 135°, and the fourth element V represents the circular polarization. The effects of the medium under investigation are applied to this vector with a 4 × 4 Mueller matrix **M** via,

$$\mathbf{S_o} = \mathbf{M} \times \mathbf{S_i}\,, \tag{1}$$

$$\begin{bmatrix} I_o \\ Q_o \\ U_o \\ V_o \end{bmatrix} = \begin{bmatrix} m_{11} & m_{12} & m_{13} & m_{14} \\ m_{21} & m_{22} & m_{23} & m_{24} \\ m_{31} & m_{32} & m_{33} & m_{34} \\ m_{41} & m_{42} & m_{43} & m_{44} \end{bmatrix} \times \begin{bmatrix} I_i \\ Q_i \\ U_i \\ V_i \end{bmatrix} = \begin{bmatrix} m_{11}I_i + m_{12}Q_i + m_{13}U_i + m_{14}V_i \\ m_{21}I_i + m_{22}Q_i + m_{23}U_i + m_{24}V \\ m_{31}I_i + m_{32}Q_i + m_{33}U_i + m_{34}V \\ m_{41}I_i + m_{42}Q_i + m_{43}U_i + m_{44}V \end{bmatrix}, \tag{2}$$

where $\mathbf{S_o}$ and $\mathbf{S_i}$ are the output and input Stokes vectors, respectively, and m_{ij} are the matrix elements. The functional forms of **M** for common interactions in clear materials are well known, so that a forward model to predict and analyze polarimetry measurements for transparent media can be readily developed. Turbidity poses significant challenges through the complications induced by multiple scattering. In addition, when several polarizations effects occur simultaneously: matrix multiplication is generally non-commutative ($\mathbf{M_A M_B} \neq \mathbf{M_B M_A}$) and, since no unique order can be assigned to simultaneous effects based on the underlying physics, the matrix-based description yields inconsistent results. An advanced approach, known as the N-matrix formalism, has been developed to tackle this non-commutative problem in clear media [31]. It makes use of differential matrices and replaces their product with a summation, which is then order-independent. We have recently extended and validated this approach in multiply scattering media, through a forward Monte Carlo-based model that can quantitatively describe the simultaneous effects of scattering, absorption, linear birefringence and optical activity [32]. This model is briefly reviewed below, as we draw upon it for validating the polar decomposition method described herein.

The outstanding challenge that we address here is the corresponding inverse problem. That is, given a particular Mueller matrix obtained from an unknown complex system, can it be analyzed to extract constituent polarization contributions? In tissue the most common polarimetry effects are depolarization, linear birefringence and optical activity [33]. These often occur simultaneously and each of these, if separately extracted from the "lumped" system Mueller matrix, holds promise as a useful biological metric. For example, chirality-induced optical rotation can be linked to the glucose concentration in the medium, and tissue structure anisotropy can be quantified by polarization birefringence measure-

ments. Here, we describe such a Mueller matrix decomposition method.

2.2. *Inverse polar decomposition analysis*

The Mueller matrix contains the combined effects of all polarizing properties of the sample. In order to isolate and quantify each effect separately, we decompose the measured matrix **M** into the product of three "basis" matrices [14, 34, 35],

$$\mathbf{M} = \mathbf{M_\Delta M_R M_D}\,, \tag{3}$$

where a depolarizing matrix $\mathbf{M_\Delta}$ accounts for the depolarizing effects of the medium, a retarder matrix $\mathbf{M_R}$ describes the effects of linear birefringence and optical activity, and a diattenuator matrix $\mathbf{M_D}$ includes the effects of linear and circular dichroism [34]. Using the known forms of these "basis" matrices, the measured **M** can be decomposed through a series of mathematical operations into the three "basis" matrices [34]. Once calculated, these constituent matrices are further analyzed to derive quantitative individual polarization medium properties (Figure 1). Lu and Chipman initially proposed this approach for optically clear media [34]. The validity of this approach in turbid media is demonstrated with both experimental and simulated data where the constituent properties are controlled and known *a priori*.

In biomedical polarimetry, three properties that are particularly important are depolarization, linear birefringence due to structural proteins (tissue anisotropy) and optical activity due to chiral molecules such as glucose. The depolarization is quantified through $\mathbf{M_\Delta}$ as the net depolarization coefficient, Δ. The measurable effects of birefringence and optical activity (linear retardance δ and optical rotation ψ respectively) are contained in $\mathbf{M_R}$. These three quantities are calculated from the elements of the 4×4 constituent matrices as [14, 34]

$$\Delta = 1 - \frac{|\mathrm{tr}\,(\mathbf{M_\Delta}) - 1|}{3}\,, \tag{4}$$

$$\delta = \cos^{-1}\left(\sqrt{(m_{\mathbf{R}22} + m_{\mathbf{R}33})^2 + (m_{\mathbf{R}32} - m_{\mathbf{R}23})^2} - 1\right), \tag{5}$$

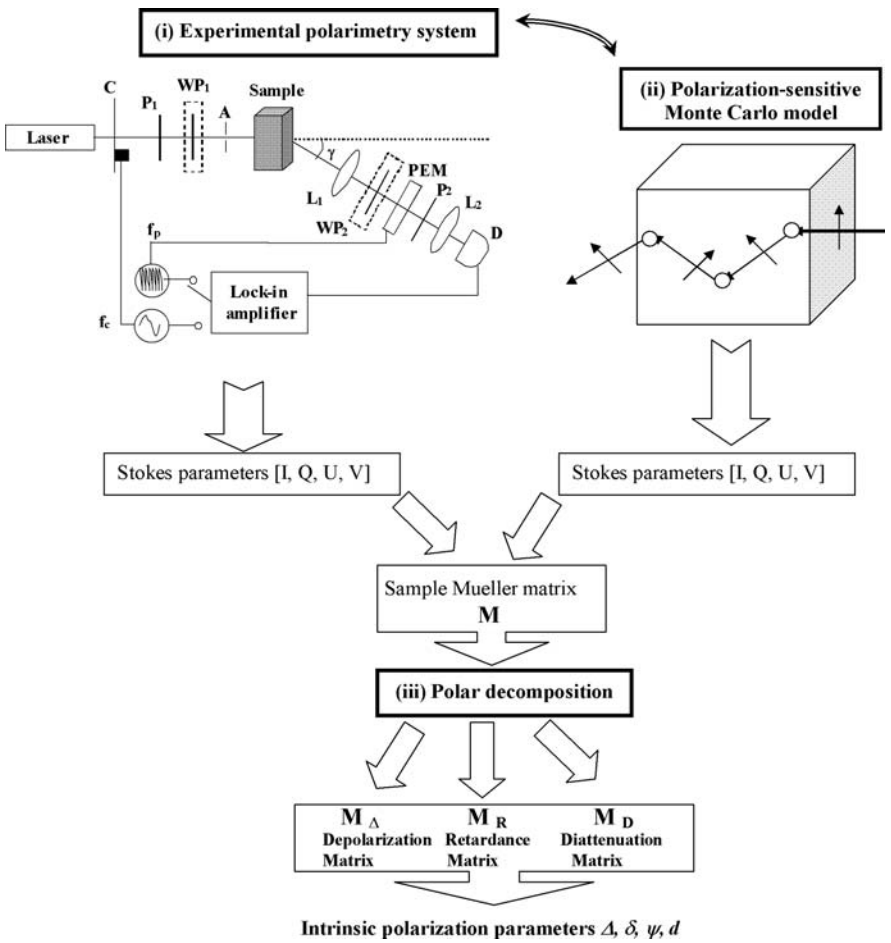

Figure 1 Schematic of the turbid polarimetry platform: **(i)** experimental system based on polarization modulation and phase-sensitive synchronous detection, **(ii)** polarization-sensitive Monte Carlo simulations for forward modeling of simultaneous polarization effects in the presence of turbidity and **(iii)** the polar decomposition of the Mueller matrix to inverse calculate the constituent polarization contributions in complex turbid media. In the experimental system **(i):** C, mechanical chopper; P_1, P_2, polarizers; WP_1, WP_2, removable quarter wave plates; A, aperture; L_1, L_2 lenses; PEM, photoelastic modulator; D, photodetector; f_c, f_p modulation frequencies of mechanical chopper and PEM, respectively. The detection optics can be rotated by an angle γ around the sample.

and

$$\psi = \tan^{-1}\left(\frac{m_{\mathbf{R}32} - m_{\mathbf{R}23}}{m_{\mathbf{R}22} + m_{\mathbf{R}33}}\right), \quad (6)$$

where $m_{\mathbf{R}ij}$ are elements of the retardance matrix $\mathbf{M_R}$. In addition, the diattenuation d, which is due to differential attenuation (absorption and scattering) of orthogonal polarizations for both linear and circular polarization states, is determined as

$$d = \frac{1}{m_{\mathbf{D}11}}\sqrt{m_{\mathbf{D}12}^2 + m_{\mathbf{D}13}^2 + m_{\mathbf{D}14}^2}, \quad (7)$$

where $m_{\mathbf{D}ij}$ are elements of the diattenutation matrix $\mathbf{M_D}$.

Note that the matrix multiplication order in Eq. (1) appears ambiguous so that 6 different decompositions are possible. However, it has been shown that the matrix product in Eq. 1 or its reverse order ($\mathbf{M} = \mathbf{M_D}\,\mathbf{M_R}\,\mathbf{M_\Delta}$) *always* leads to a physically realizable Mueller matrix [34]. Most importantly, the derived polarization parameters particularly useful in tissue characterization, Δ, δ, and ψ, are independent of the multiplication order of the basis matrices in Eq. (1) [34].

2.3. Polarimetry system

For experimental studies, we use a polarization modulation and phase-sensitive synchronous detection approach to measure the small polarization signals in a large depolarized background, as summarized in Figure 1. The details have been reported previously [15, 32]. Briefly, for this particular configuration, the polarization states are controlled using a polarizer and quarter wave-plate combination, enabling either linear or circular incidence. After interacting with the sample, the partially depolarized beam in a user-selected direction (angle γ) is modulated using a linearly-birefringent resonant photoelastic modulator (PEM). The light then passes through an analyzer, converting the polarization modulation to intensity modulation detectable by a photodetector. The resultant photocurrent is fed into a lock-in amplifier synchronous with the PEM modulation frequency for high signal to noise ratio (SNR) detection of the surviving polarization states. The Stokes vector of the output light is directly measured using the first and second harmonics of the lock-in detected signals [15, 32]. The complete Mueller matrix can be obtained by cycling the input polarization between four states (linear polarization at 0°, 45°, 90°, and right circular polarization), measuring the output Stokes vector for each respective input state, and performing simple algebraic manipulations [34]. Similar systems with electronically driven optical polarization modulators have demonstrated long-term instability caused by thermal effects [36, 37]. However, testing our system over extended periods of time (~hours) have shown that once warmed up (~10 min of operation), it is reasonably resistant to such instability.

For the experimental system, solid optical phantoms were developed using polyacrylamide as a base medium, with polystyrene microspheres to create turbidity, sucrose to induce optical activity, and mechanical stretching to cause linear birefringence allowing full experimental control of all constituent effects. The model allows for generation of Mueller matrices for media of any given properties.

2.4. Monte Carlo model

In addition to experimental polarimetry suitable for highly turbid media, we have also developed and validated a forward model for polarized light propagation in turbid media, using a Monte Carlo computational model [32, 38]. This statistical formalism, although less rigorous than the electromagnetic field modeling based on Maxwells equations, is well suited for describing light interactions with complex random media, and can be extended to include polarimetric descriptors [11, 39–41]. Our polarization-sensitive Monte Carlo model has been further extended to simulate simultaneous polarization effects in the presence of turbidity, employing the above-mentioned N-matrix formalism [31]. This is particularly important for simulation of biological tissue that often exhibits several polarization effects simultaneously. In the simulation, many photons (10^7–10^9) are tracked individually as they propagate and scatter through the media. Their fates are simulated using known single-interaction effects, applied in a statistical sense until they are absorbed or leave the media of interest. Repeating this process many times and keeping track of the resultant cumulative values generates quantities of interest such as Stokes vectors, Mueller matrices, pathlength distributions, and sampling volumes. The various polarizing effects of the medium are applied to the photons between scattering events. The Monte Carlo model has proven to be invaluable for data analysis, system validation, and guidance/design of experimental systems [42].

2.5. Myocardial samples

To investigate the use of this methodology for monitoring regenerative treatments of myocardial infarction, myocardial samples from a rat model of myocardial infarction and regeneration were used. All animal studies were carried out under institutional approval from the University Health Network, Toronto, Canada. The heart samples were obtained in an established

model in which myocardial infarction was induced in Lewis rats through coronary artery ligation. Mesenchymal stems cells transfected with human elastin gene were administered to the treatment group by intramyocardial injection at the site of infracted two weeks after the ligation procedure. Both the control ($n = 4$) and treatment ($n = 4$) groups were sacrificed after four weeks and the hearts were removed and fixed in 10% formalin. Finally, the fixed heart samples were sectioned into one mm thick axial slices and examined with the turbid polarimeter. It must be noted that although the tissue fixation process may alter the polarization properties of the tissue due to the cross-linking, it was required for tissue sectioning. The potential effects of the formalin fixation, and ways of eliminating it, are currently being investigated and will be reported in a forthcoming publication.

3. Results and discussion

3.1. Theoretical and experimental validation

This extended Mueller matrix decomposition methodology has seen only initial use in turbid media [14, 43], but has not been rigorously validated. Experimental validation was completed using the previously described polyacrylamide phantom system [32]. Table 1 shows the Mueller matrix measured in a turbid media and the corresponding decomposed $\mathbf{M_\Delta}$, $\mathbf{M_R}$ and diattenuation $\mathbf{M_D}$ matrices. This medium mimics the complexity of biological tissues, in that it exhibits linear birefringence (sample extension by 2 mm for strain applied along the vertical direction), chirality (concentration of 1 M of sucrose corresponding to magnitude of optical activity of $\chi = 1.96°/\text{cm}$), and turbidity (1.4 μm diameter polystyrene microspheres, resulting in a scattering coefficient of $\mu_s = 30\ \text{cm}^{-1}$ and anisotropy parameter $g = 0.95$ at $\lambda = 633$ nm). The measurement was performed in the forward direction ($\gamma = 0°$ in Figure 1) through a $1 \times 1 \times 4$ cm phantom. The complicated nature of the resultant Mueller matrix $\mathbf{M}$, with essentially all 16 non-zero matrix elements being non-zero, highlights the challenge of extracting useful sample parameters from this complex intertwined information. In contrast, the three basis matrices derived from the decomposition procedure exhibit simpler structures with many zero off-diagonal elements, and are directly amenable to further analysis. Eqs. (2)–(5) were applied to the decomposed basis matrices to retrieve the individual polarization parameters (δ, ψ, Δ and d). These are listed in Table 1, showing excellent agreement with the input values (within ±5% for all parameters).

Table 1 *Top:* The experimentally recorded Mueller matrix and the decomposed matrices for a birefringent (extension = 2 mm), chiral (concentration of sucrose = 1 M, $\chi = 1.96°/\text{cm}$), turbid ($\mu_s = 30\ \text{cm}^{-1}$, $g = 0.95$) phantom. *Bottom:* The values for the polarization parameters extracted from the decomposed matrices via Eqs. (2)–(5) (2nd column). The input control values for linear retardance δ and optical rotation ψ (3rd column) were obtained from measurement on a clear ($\mu_s = 0\ \text{cm}^{-1}$) phantom having the same extension (2 mm) and similar concentration of sucrose (1 M) as that of the turbid phantom, and corrected for the increased pathlength due to multiple scattering (determined from Monte Carlo modeling). The expected value for the depolarization coefficient Δ was determined from the Monte Carlo simulation of the experiment.

$$\mathbf{M} = \begin{pmatrix} 1.0000 & 0.0185 & 0.0029 & 0.0042 \\ 0.0172 & 0.7569 & -0.0405 & 0.0462 \\ 0.0034 & 0.0524 & 0.5450 & -0.5466 \\ 0.0024 & -0.0070 & 0.6244 & 0.5967 \end{pmatrix}$$

$$\mathbf{M_\Delta} = \begin{pmatrix} 1.0000 & 0 & 0 & 0 \\ 0.0031 & 0.7577 & 0 & 0 \\ 0.0031 & 0 & 0.7745 & 0 \\ -0.0017 & 0 & 0 & 0.8647 \end{pmatrix} \quad \mathbf{M_R} = \begin{pmatrix} 1.0000 & 0 & 0 & 0 \\ 0 & 0.9972 & -0.0470 & 0.0578 \\ 0 & 0.0742 & 0.6964 & -0.7138 \\ 0 & -0.0067 & 0.7161 & 0.6980 \end{pmatrix} \quad \mathbf{M_D} = \begin{pmatrix} 1.0000 & 0.0185 & 0.0029 & 0.0042 \\ 0.0185 & 1.0000 & 0.0000 & 0.0000 \\ 0.0029 & 0.0000 & 0.9998 & 0.0000 \\ 0.0042 & 0.0000 & 0.0000 & 0.9998 \end{pmatrix}$$

Parameters	Input control values	Estimated values
Linear retardance (δ)	0.83 rad	0.79 rad
Optical rotation (ψ)	2.14°	2.05°
Depolarization coefficient (Δ)	0.19	0.21
Diattenuation (d)	0	0.02

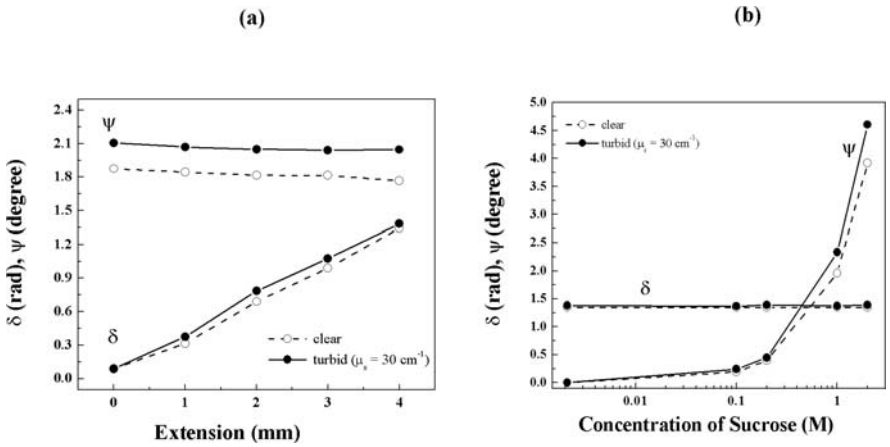

Figure 2 (**a**) Linear retardance, δ, and optical rotation, ψ, estimated from the decomposition of experimentally recorded Mueller matrices from solid chiral phantoms ($\chi = 1.96°$/cm, corresponding to 1 M concentration of sucrose) with varying degrees of strain-induced birefringence (extension of 0–4 mm, $\delta = 0$–1.345). Results are shown for both clear ($\mu_s = 0\ \text{cm}^{-1}$) and turbid ($\mu_s = 30\ \text{cm}^{-1}$, $g = 0.95$) phantoms. The measurements were performed in the forward direction ($\gamma = 0°$) through a $1 \times 1 \times 4$ cm phantom.
(**b**) δ and ψ estimated from the decomposition of Monte Carlo-generated Mueller matrices from birefringent media (linear birefringence $\Delta n = 1.36 \times 10^{-5}$, corresponding to $\delta = 1.345$ rad [4 mm phantom extension] for a path length of 1 cm, Δn is anisotropy in refractive indices, the difference in refractive index along the extraordinary axis and the ordinary axis) having varying levels of chirality ($\chi = 0$, 0.196, 0.392, 1.96 and 3.92°/cm, corresponding to concentration of sucrose of 0, 0.1, 0.2, 1 and 2 M, respectively). Results are shown for both clear ($\mu_s = 0\ \text{cm}^{-1}$) and turbid ($\mu_s = 30\ \text{cm}^{-1}$, $g = 0.95$) media.

The values for δ and ψ determined from the decomposition of the measured Mueller matrices in both clear ($\mu_s = 0\ \text{cm}^{-1}$) and turbid ($\mu_s = 30\ \text{cm}^{-1}$, $g = 0.95$) optically active ($\chi = 1.96°$/cm) phantoms with increasing birefringence (sample extension of 0–4 mm, $\delta = 0$–1.345 rad), are shown in Figure 2A. This is an illustrative data set for forward-detection geometry only ($\gamma = 0°$ in Figure 1); investigations using other detection directions are in progress, since these may be more relevant in some specific biomedical applications. Again, the values from both clear and scattering samples are in close agreement with the controlled experimental inputs ($\psi \approx 1.96°$ and $\delta \approx 1.345$ rad at 4 mm of extension). Further, the similarity of the derived retardance and optical rotation in both clear and scattering media suggests that the depolarizing effects of multiple scattering have been properly isolated. The small increases in both linear retardance and optical rotation in the presence of turbidity are caused by the increase in optical pathlength due to multiple scattering, resulting in slight accumulations of δ and ψ values (at least for this $\gamma = 0°$ detection geometry [34]). Figure 2B shows the derived linear retardance δ and optical rotation ψ parameters, using Monte Carlo generated Mueller matrices, and with the chiral molecule concentration as an independent variable. Again, both the clear and turbid values compare well with the input parameter values ($\delta \approx 1.4$ rad and $\psi \approx 1.96°$ at 1 M sucrose), demonstrating the self-consistency of the decomposition analysis and successful decoupling of the effects. Note that none of these trends could be gleaned from the lumped Mueller matrix, where at best one would have to resort to semi-empirical comparison of changes in selected matrix elements, which contain contributions from several effects [15, 32]. Derivation and quantification of the absolute linear retardance δ and optical rotation ψ values is enabled exclusively by the decomposition analysis. Based on these and other continuing studies [43], this approach seems to be valid for complex turbid media, and so may be applicable to studies of biological tissues, which is our primary goal.

3.2. Determining intrinsic optical activity: measurement of glucose in tissue

An example of an important biomedical application is the quantification of the small optical rotations due to blood glucose in diabetic patients. Several different optical-based techniques have been investigated for this application, but none have provided a clinically useful solution to date [44]. The optical rotation due to glucose being a chiral molecule may, in principle, provide the sensitivity and specificity required. However, a major stumbling block is that the optical rotation due to chiral substances is swamped by the much larger changes in the orientation angle of the polarization vector due to scattering [15]. Hence, it is thus essential to isolate the optical rotation caused exclusively by glucose (or other chiral molecules of interest) from this background apparent rotation. The

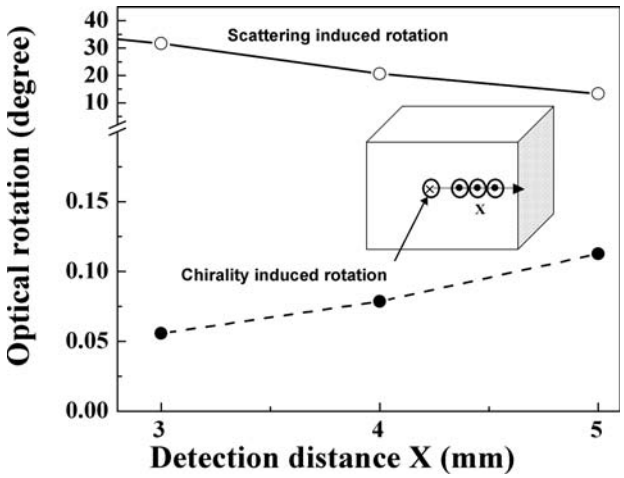

Figure 3 Calculated optical rotation, ψ (derived from the decomposition of Monte Carlo generated Mueller matrices: solid circles), of scattered light emerging in the backscattering direction as a function of distance from the center of the incident beam in a chiral ($\chi = 0.082°$/cm, corresponding to 100 mM concentration of glucose) isotropic turbid medium ($\mu_s = 30\ \text{cm}^{-1}$, $g = 0.95$, thickness $t = 1$ cm). The corresponding scattering-induced rotation of the polarization vector derived from the Stokes parameters of scattered light (for incident Stokes vector $[1\ 0\ 1\ 0]^T$) is shown by open circles. The inset shows the backwards detection geometry. The chirality-induced rotation approaches zero in the exact backscattering direction ($X = 0$, data not shown).

above matrix decomposition methodology can perform this task, as shown in Figure 3. This shows the variation in the derived optical rotation ψ in the backward direction ($\gamma \sim 180°$, a geometry that is convenient for *in vivo* applications) as a function of the distance from the center of an incident beam in a chiral turbid medium ($\chi = 0.082°$/cm, corresponding to 100 mM concentration of glucose, $\mu_s = 30\ \text{cm}^{-1}$, $g = 0.95$, thickness = 1 cm). As can be seen, changes in the polarization caused by scattering are manifest as large apparent optical rotations [14, 15]. Decomposition analysis reveals that the effect is due to linear diattenuation (the difference in amplitude between the scattered light that is polarized parallel to and perpendicular to the scattering plane). This confounding effect is due mainly to the backscattered photons and gradually decreases as one goes away from the exact backscattering direction.

Decomposition of the Mueller matrix can thus decouple the irrelevant (chirality-unrelated) rotation from the much smaller ψ rotation values caused by the circular birefringence of the medium. In combination with photon path-length distributions from Monte Carlo simulations [42], we are currently investigating methods for extracting the true chiral molecule concentrations from derived optical rotations. Spectroscopic-based polarimetry combined with chemometric regression analysis [45] is being investigated to isolate the rotation due to glucose from that caused by other chiral constituents [44].

3.3. Myocardial tissue monitoring for regenerative treatments

The anisotropic organized nature of many tissues that stems from their fibrous structure leads to linear birefringence (or linear retardance), manifest as anisotropic refractive indices parallel and perpendicular to the fibers. Muscle fibers and extra-cellular matrix proteins (such as collagen and elastin) exhibit such linear birefringence [33]. Changes in this anisotropy resulting from disease progression or treatment response can alter the optical birefringence properties, making this parameter a potentially sensitive probe of tissue status. For example, upon suffering an infarction, a portion of the myocardium is deprived of oxygenated blood and subsequently cardiomyocytes die, being replaced by the fibrotic (scar) tissue [46]. Current methods to characterize the structure of the myocardium measure mechanical changes (e.g., elastography [47]) or electrical changes (e.g., impedance [48]). Recently, stem cell based regenerative treatments for myocardial infarction have been shown to reverse these trends by increasing the muscular and decreasing the scar tissue components [49–51]. These remodeling processes likely affect tissue structural anisotropy, and polarized light may offer a sensitive probe into the state of the myocardium after infarction and report on the success of regenerative treatments. This could be an invaluable quantitative and objective research tool in animal models and could be implemented via fiber-optic catheters in patients. As in other applications, these small birefringence alterations must be decoupled from the other confounding polarization effects that are present in the composite signals of the measured Mueller matrix elements.

Using the experimental turbid polarimetry set-up shown in Figure 1, we measured the Mueller matrices in transmission mode through 1-mm thick *ex vivo* myocardial samples from Lewis rats harvested after myocardial infarction, both with and without stem cell treatments. These were analyzed by the decomposition method to obtain δ values (Figure 4). A large decrease in linear retardance is seen in the infarcted region of the untreated myocardium (Figure 4a) due to the native, well-ordered anisotropic structure being replaced by disorganized isotropic scar tissue. An increase in δ towards the native (pre-infarct) in levels is seen in animals receiving stem cell therapy (Figure 4b) which leads to re-growth and re-organization of the damaged tissue, as indicated by the increased retardance levels. Shown in the bar graph of Figure 4c

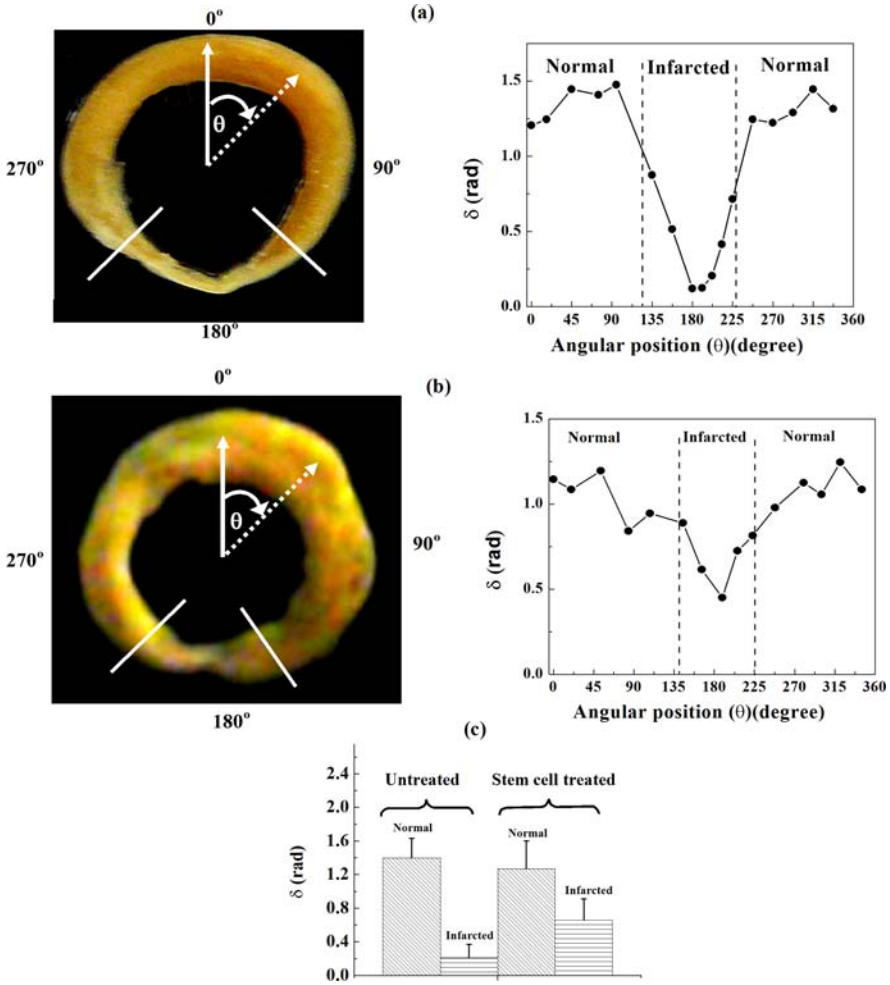

Figure 4 (online colour at: www.biophotonics-journal.org) Linear retardance δ derived from transmission polarization measurements in 1-mm-thick sections from Lewis rat hearts following myocardial infarction. (**a**) untreated tissues, (**b**) tissues following stem-cell treatments. The marked sector around $\theta = 180°$ indicates the infracted region. Decreased birefringence levels in the infarcted region compared to normal regions are seen; this difference in reduced following stem-cell therapy as infracted region retardance values increase towards normal-tissue levels. The results from birefringence measurements from the controls and the stem-cell treated groups of infracted hearts are shown in histogram form in (**c**). Error bars represent the standard deviation. Both untreated and stem-cell treated groups were comprised of 4 hearts and 5 measurements were preformed in each region (normal and infarcted).

are the mean linear retardance values from measurements of treated and untreated heart groups in the infarcted and normal regions. Statistically significant ($p = 0.03$) differences in derived retardance values exist between normal and infracted regions, and between infracted regions with and without stem-cell treatments. An increase in retardance in the infarcted regions of the treated hearts indicates reorganization and re-growth, as confirmed by a histologic examination. Of interest to note in these tissue measurements is that light absorption was present [52], as opposed to the phantom and Monte Carlo studies which had no absorption. While absorption does not affect the decomposition process, it does influence the polarization parameters. This is due to the reduction in the average optical pathlength through the medium (due the preferential absorption of longer path photons), resulting in different polarization values relative to a similar non-absorbing medium (specifically, lower values of optical rotation and retardance and higher surviving degree of polarization).

These intial *ex vivo* studies demonstrate the potential of polarimetric moitoring of myocardial tissues following stem cell therapy. Current work is directed towards developing an *in vivo* measurement system based on these principles using diffusely reflected light.

4. Conclusions

A Mueller matrix polar decomposition methodology has been validated and explored in chiral birefringent turbid media, including biological tissues. The individual polarization effects can be successfully decoupled and quantified, despite their simultaneous occurrence, even in the presence of the numerous complexities due to multiple scattering. This opens the door for a variety of powerful, noninvasive polarimetry-based techniques for biomedical applications, of which we have illustrated two important examples.

Acknowledgements This work was supported by the National Sciences and Engineering Research Council of Canada. We thank Dr. Daniel Côté for assistance with the Monte Carlo software and Dr. Xinxin Guo for assistance with the experimental system.

Nirmalya Ghosh, PhD is a physicist by training, with further specialization in biomedical optics, spectroscopy and biophotonics. He completed his M.S. in Physics from University of Kalyani, India and M. Tech. in Laser Technology from IIT Kanpur, India. He then joined Laser Biomedical Applications & Instrumentation Division (LBAID), Raja Ramanna Centre for Advanced Technology (RRCAT), Indore, Department of Atomic Energy (DAE), India as a scientist, where he started his research on biomedical applications of lasers. He completed his PhD in Physics from RRCAT, India and his thesis research was focused on understanding depolarization of light in a complex turbid medium like biological tissue and evaluating its use for biomedical imaging and diagnosis. At present he is conducting postdoctoral research in the field of biophotonics (with particular emphasis on tissue polarimetry) with Department of Medical Biophysics at the University of Toronto. He has published over twenty five papers in peer-reviewed journals, fifteen articles in edited volumes, and book chapters in the area of biomedical optics, spectroscopy and biophotonics.

Michael Wood completed his undergraduate degree in Computer Engineering at the University of Western Ontario in 2004. Currently he is pursuing his PhD in Medical Biophysics at the University of Toronto where his work focuses on the use of polarized light for tissue characterization. He is the recipient of a postgraduate scholarship from the National Science and Engineering Research Council of Canada. He has 11 scientific publications and one book chapter.

Shu-Hong Li is a laboratory technician and manager in the Department of Cardiovascular research at the Toronto General Hospital. She received her masters in pharmaceutical sciences from the University of British Columbia in 2000. As part of Dr. Li's laboratory, her work is focused on finding optimal cell types for transplantation in the myocardium, and describing the optimal conditions under which the transplanted cells can achieve the most efficient repair.

Richard Weisel, MD is the Director of the Toronto General Research Institute. Improving quality of life for the cardiac patient has been a lifelong pursuit for Dr. Weisel. A graduate of Yale, Dr. Weisel received his training in Milwaukee and Boston, joining Toronto General Hospital in 1976. Since then, this preeminent clinician scientist has contributed to cardiology science through innovative research, international lectures, publications, and life-saving expertise as a cardiovascular surgeon. His major research interests lie in cell transplantation, myocardial protection and vascular biology. He has published over 300 publications in peer-reviewed journals and was a recipient of the Ontario Heart & Stroke Foundation's Career Investigator award for six consecutive years.

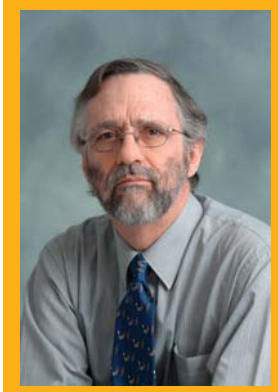

Brian C. Wilson, PhD was appointed Professor of Medical Biophysics and Head of the Division of Biophysics and Bioimaging at the Ontario Cancer Institute/Faculty of Medicine, University of Toronto in 1993. A graduate in particle physics from Glasgow University, he worked at the Institute of Cancer Research in London and then in Australia before moving to McMaster University in Canada in 1981, where he initiated a research program in translational and clinical biophotonics. He heads the biophotonics program of the Canadian Institute for Photonic Innovations, has held Visiting Professor positions at Harvard University and University of Sao Paulo, Brazil and is currently Professor-at-Large, University of Western Australia. He is co-founder of 2 start-up companies, with a 3rd on the way. He has published over 300 scientific papers and trained 50+ graduate students and fellows.

Ren-Ke Li, MD, PhD is a Professor of Medicine in the Department of Surgery, Division of Cardiovascular Surgery and Department of Laboratory Medicine and Pathobiology at the University of Toronto and a Senior Scientist at the Toronto General Research Institute, University Health Network. He is the recipient of the Canada Research Chair in Cardiac Regeneration and a Career Investigator of the Heart and Stroke Foundation of Canada. Dr. Li has been on the forefront in the field of cell transplantation and tissue engineering. In 1996, he published the first demonstration that cells transplanted into myocardial scar tissue survived, differentiated into muscle tissue, and improved heart function. More recently, his group has defined optimal cell types for transplantation, and described the optimal conditions under which the transplanted cells can achieve the most efficient repair. Currently, they are attempting to determine the mechanisms by which transplanted cells exert their beneficial effects. Dr. Li has published 129 peer-reviewed papers.

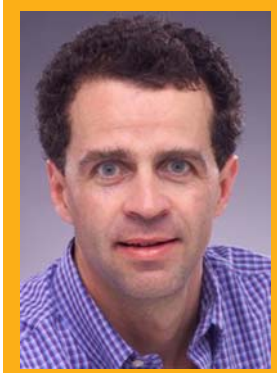

Alex Vitkin, PhD is an engineering physicist/biomedical engineer specializing in medical physics and the application of lasers in medicine. He is currently a professor of medical biophysics and radiation oncology at the University of Toronto, a senior scientist in the division of biophysics and bioimaging at the Ontario Cancer Institute, and a clinical medical physicist at Princess Margaret Hospital (all in Toronto, Ontario, Canada). His research is in the field of biophotonics, with particular emphasis on Doppler optical coherence tomography, tissue polarimetry, and optical fiber sensors.
Dr. Vitkin has published over 90 scientific papers in peer-reviewed literature. He has served as the Guest Editor (Biophysics) for the Journal of Applied Physics, and is currently a topical editor of Optics Letters.

References

[1] V. Ronchi, The Nature of Light (Harvard University Press, Cambridge, Massachusetts, 1970).
[2] J. Michl and E. W. Thulstrup, (Spectroscopy with Polarized Light (VCH, New York, 1986).
[3] R. A. Hegstrom and D. K. Kondepudi, The handedness of the universe, Scientific American January 108–115 (1990).
[4] C. A. Browne and F. W. Zerban, Physical and Chemical Methods of Sugar Analysis (Wily, New York, 1941).
[5] B. Jirgensons, Optical Rotatory Dispersion of Proteins and Other Macromolecules (Springer-Verlag, 1960).
[6] D. S. Kliger, J. W. Lewis, and C. E. Randall, Polarized Light in Optics and Spectroscopy (Academic Press–Harcourt Brace Jovanovich, New York, 1990).
[7] C. Brouseau, Fundamentals of Polarized Light a Statistical Approach (Wiley Interscience, 1998).
[8] M. Gadsden, P. Rothwell, and M. J. Taylor, Detection of circularly polarized-light from noctilucent clouds, Nature **278**, 628–629 (1979).
[9] A. Chrysostomou, P. W. Lucas, and J. H. Hough, Circular polarimetry reveals helical magnetic fields in the young stellar object HH 135–136, Nature **450**, 71–73 (2007).
[10] R. S. Gurjar, V. Backman, L. T. Perelman, I. Georgakoudi, K. Badizadegan, I. Itzkan, R. R. Dasari, and M. S. Feld, Imaging human epithelial properties with polarized light scattering spectroscopy, Nature Medicine **7**, 245–1249 (2001).
[11] V. V. Tuchin, L. Wang, and D. À. Zimnyakov, Optical Polarization in Biomedical Applications (Springer-Verlag, 2006).
[12] N. G. Khlebtsov, I. L. Maksimova, V. V. Tuchin, and L. Wang, Introduction to Light Scattering by Biological Objects, in: Handbook of Optical Biomedical Diagnostics, Vol. PM107, edited by V. V. Tuchin (SPIE Press, Bellingham, WA, 2002), chap. 1, pp. 31–167.
[13] M. Xu and R. R. Alfano, Random walk of polarized light in turbid media, Physical Review Letters **95**, 2139001 (2005).
[14] S. Manhas, M. K. Swami, P. Buddhiwant, N. Ghosh, P. K. Gupta, and K. Singh, Mueller matrix approach for determination of optical rotation in chiral turbid media in backscattering geometry, Optics Express **14**, 190–202 (2006).
[15] X. Guo, M. F. G. Wood, and I. A. Vitkin, Angular measurement of light scattered by turbid chiral media using linear Stokes polarimetry, Journal of Biomedical Optics **11**, 041105 (2006).
[16] K. Sokolov, R. Drezek, K. Gossage, and R. Richards-Kortum, Reflectance spectroscopy with polarized light: is it sensitive to cellular and nuclear morphology? Optics Express **5**, 302–317 (1999).
[17] S. L. Jacques, J. C. Ramella-Roman, and K. Lee, Imaging skin pathology with polarized light, Journal of Biomedical Optics **7**, 329–340 (2002).

[18] V. Sankaran, J. T. Walsh, and D. J. Maitland, Comparative study of polarized light propagation in biologic tissues, Journal of Biomedical Optics **7**, 300–306 (2002).
[19] M. Bartlett, G. Huang, L. Larcom, and H. Jiang, Measurement of particle size distribution in mammalian cells in vitro by use of polarized light spectroscopy, Applied Optics **43**, 1296–1307 (2004).
[20] M. J. Rakovic, G. W. Kattawar, M. Mehruübeoglu, B. D. Cameron, L. V. Wang, S. Rastegar, and G. L. Coté, Light backscattering polarization patterns from turbid media: theory and experiment, Applied Optics **38**, 3399–3408 (1999).
[21] A. H. Hielscher, J. R. Mourant, and I. J. Bigio, Influence of particle size and concentration on the diffuse backscattering of polarized light from tissue phantoms and biological cell suspensions, Applied Optics **36**, 125–135 (1997).
[22] J. M. Schmitt, A. H. Gandjbakhche, and R. F. Bonner, Use of polarized light to discriminate short-path photons in a multiply scattering medium, Applied Optics **31**, 6535–6546 (1992).
[23] M. Dogariu and T. Asakura, Photon pathlength distribution from polarized backscattering in random media, Optical Engineering **35**, 2234–2239 (1996).
[24] W. S. Bickel, J. F. Davidson, D. R. Huffman, and R. Kilkson, Application of polarization effects in light scattering: a new biophysical tool, Proceedings of the National Academy of Sciences **73**, 486–490 (1976).
[25] I. A. Vitkin, R. D. Laszlo, and C. L. Whyman, Effects of molecular asymmetry of optically active molecules on the polarization properties of multiply scattered light, Optics Express **10**, 222–229 (2002).
[26] R. C. N. Studinski and I. A. Vitkin, Methodology for examining polarized light interactions with tissues and tissue-like media in the exact backscattering direction, Journal of Biomedical Optics **5**, 330–337 (2000).
[27] I. A. Vitkin, and E. Hoskinson, Polarization studies in multiply scattering media, Optical Engineering **39**, 353–362 (2000).
[28] D. Côté and I. A. Vitkin, Balanced detection for low-noise precision polarimetric measurements of optically active, multiply, scattering tissue phantoms, Journal of Biomedical Optics **9**, 213–220 (2004).
[29] K. C. Hadley and I. A. Vitkin, Optical rotation and linear and circular depolarization rates in diffusely scattered light from chiral, racemic, and achiral turbid media, Journal of Biomedical Optics **7**, 291–299 (2002).
[30] D. Goldstein, Polarized Light (Marcel Decker Inc., 2003).
[31] R. C. Jones, New calculus for the treatment of optical systems. VII. Properties of the N-matrices, Journal of the Optical Society of America **38**, 671–685 (1948).
[32] M. F. G. Wood, X. Guo, and I. A. Vitkin. Polarized light propagation in multiply scattering media exhibiting both linear birefringence and optical activity: Monte Carlo model and experimental methodology, Journal of Biomedical Optics **12**, 014029 (2007).
[33] L. V. Wang, G. L. Coté, and S. L. Jacques, Editors, Special Section on Tissue Polarimetry, Journal of Biomedical Optics **7**, 278–397 (2002).
[34] 34. S. Y. Lu and A. Chipman, Interpretation of Mueller matrices based on polar decomposition, Journal of the Optical Society of America A **13**, 1106–1113 (1996).
[35] J. Morio and F. Goudail, Influence of the order of diattenuator, retarder, and polarizer in polar decomposition of Mueller matrices, Optics Letters **29**, 2234–2236 (2004).
[36] R. G. Johnson, S. B. Singham, and G. C. Salzman, Polarized Light Scattering, Comments Mol. Cell. Biophys. **5**, 171–192 (1988).
[37] G. C. Salzmann, S. B. Singham, R. G. Johnson, and C. F. Bohren, Light Scattering and Cytometry, in: Flow Cytometry and Sorting, 2nd ed., edited by M. R. Melamed, T. Lindmo, and M. L. Mendelsohn (Wiley-Liss, New York, 1990), pp. 81–107.
[38] 38. D. Côté and I. A. Vitkin, Robust concentration determination of optically active molecules in turbid media with validated three-dimensional polarization sensitive Monte Carlo calculations, Optics Express **13**, 148–163 (2005).
[39] L. V. Kuzmin, I. V. Meglinski, and Churmakov, Coherent effects in multiple scattering of linearly polarized light, Optics and Spectroscopy **98**, 653–659 (2005).
[40] F. Jaillon and H. Saint-Jalmes, Description and time reduction of a Monte Carlo code to simulate propagation of polarized light through scattering media, Applied Optics **42**, 3290–3296 (2003).
[41] W. Wang and L. V. Wang, Propagation of polarized light in birefringent media: A Monte Carlo study, Journal of Biomedical Optics **7**, 350–358 (2002).
[42] X. Guo, M. F. G. Wood, and I. A. Vitkin, Monte Carlo study of path length distribution of polarized light in turbid media, Optics Express **15**, 1348–1360 (2007).
[43] N. Ghosh, M. F. G. Wood, and I. A. Vitkin, Simultaneous determination of linear retardance and optical rotation in birefringent, chiral, turbid medium using Mueller matrix polarimetry: combined Monte Carlo and experimental methodology, Journal of Biomedical Optics **13**, 044037 (2008).
[44] R. J. McNichols and G. L. Coté, Optical glucose monitoring in biological fluids: an overview, Journal of Biomedical Optics **13**, 044036 (2008).
[45] M. F. G. Wood, D. Côté, and I. A. Vitkin, Combined optical intensity and polarization methodology for analyte concentration determination in simulated optically clear and turbid biological media, Journal of Biomedical Optics, in press (2008).
[46] Y. Sun, J. Q. Zhang, J. Zhang, and S. Lamparter, Cardiac remodeling by fibrous tissue after infarction, Journal of Laboratory and Clinical Medicine **135**, 316–323 (2000).
[47] E. E. Konofaguo, J. Dhoogle, and J. Ophirm, Myocardial elastography – a feasibility study in vivo, Ultrasound in Medicine and Biology **28**, 475–482 (2002).
[48] M. A. Fallert, M. S. Mirotznik, S. W. Downing, E. B. Savage, K. R. Foster, M. E. Josephson, and D. K. Bogen, Myocardial electrical impedance mapping of is-

chemic sheep hearts and healing aneurysms, Circulation **87**, 199–207 (1993).

[49] D. Orlic, J. Kajstura, S. Chimenti, I. Jackoniuk, S. M. Anderson, B. Li, J. Pickel, K. MacKay, B. Nadal-Ginard, D. M. Bodine, A. Leri, and P. Anversa, Bone marrow cells regenerate infarcted myocardium, Nature **410**, 701–705 (2001).

[50] M. Jain, H. DerSimonian, D. A. Brenner, S. Ngoy, P. Teller, A. S. B. Edge, A. Zawadzka, K. Wetzel, D. B. Sawyer, W. S. Colucci, C. S. Apstein, and R. Liao, Cell therapy attenuates deleterious ventricular remodeling and improves cardiac performance after myocardial infarction, Circulation **103**, 1920–1927 (2001).

[51] X. Xu, Z. Xu, Y. Xu, and C. Cui, Selective down-regulation of extracellular matrix gene expression by bone marrow derived stem cell transplantation into infarcted myocardium, Circulation Journal **69**, 1275–1283 (2005).

[52] W. F. Cheong, S. A. Prahl, and A. J. Welch, A review of the optical properties of biological tissues, IEEE J. Quant. Electr. **26**, 2166–2185 (1990).

